中國機械工程學刊第四十二卷第一期第 93~100 頁(民國一百一十年)
Journal of the Chinese Society of Mechanical Engineers, Vol.42, No.1, pp 93~100 (2021)

A Practical Approach for Analysis of Effect of the Oil Temperature and Size Variation on the Steady-state Performance of the Bent axis Hydro-Motors

Ajit Pandey*, Amit Kumar**, Anupam Alok***
Alok Vardhan****, Kabir Dasgupta*****

Keywords: Bent axis hydro-motor, Flow-loss, Torque loss, Oil temperature, Overall efficiency.

ABSTRACT

Hydraulic motor of bent axis design are commonly used in heavy earth moving machinery, mining industries and construction equipment due to their high efficiency and wider torque speed ranges. The present work is conducted in order to study the effect of oil temperature and size variations on the steady-state performances of the fixed displacement bent axis hydro-motors under a specific operating condition. In this respect, five different capacities of the fixed displacement bent axis hydro-motor (10 cc through 28 cc) are considered. The effects of the operating conditions such as oil temperature, sizes of the motor, constant load and speed on its flow and torque-losses are identified. The outcome of them on the performance of the hydro-motor is characterized.

From the test data, the characteristic of the various losses co-efficient are identified. A mathematical model of the losses is established that takes into account the influences of the oil temperature, capacities of hydro-motor. Using the said model, the overall efficiency, torque loss and the slip of the different capacities hydro-motor at five different operating temperature (40□C through 80□C) are compared.

It is concluded that with increase in the temperature and sizes of hydro motor, the overall performance of the hydro-motors increases. Such model may be used to describe the performance of the various sizes of hydro-motor for wide range of operating temperature. The proposed model may be useful for the practicing engineers to select the bent axis hydro-motor drive for a given application in mining industries and construction equipment.

Paper Received June, 2019. Revised December, 2020. Accepted January, 2021, Author for Correspondence: Ajit Pandey
**Department of Mechanical Engineering, NIT, PATNA (India) Email:ajit.saurabh100@gmail.com*
***Department of Mechanical Engineering, NIT, PATNA (India) Email: amit@nitp.ac.in*
****Department of Mechanical Engineering, NIT, PATNA (India) Email: anupamalok59@gmail.com*
*****Department of Mining Machinery Engineering, Indian School of Mines, Dhanbad (India) Email: alok.or.monu@gmail.com*
******Department of Mining Machinery Engineering, Indian School of Mines, Dhanbad (India) Email:dasgupta_k2001@yahoo.co.in*

INTRODUCTION

For heavy-duty high pressure applications the hydro-motor of bent axis design are frequently used in hydrostatic (HST) drives. Such motors are extensively observed in mobile hydraulics to propel drive of off road vehicles, in excavator for its swing motion, forest machinery as saw motor and various other applications. Such hydro-motor has a promising prospect in the application of the hydraulic drives that require simple and compact structure. While analyzing the hydro-motor performance, it is important to consider its various losses. The losses of the pump and the hydro-motor have detrimental effects on the overall efficiency of the hydraulic drive. In recent decades, various approaches have been suggested by notable researchers to describe the losses of the hydrostatic components. Zarotii et al. have addressed an automatic procedure to define the sizes of the pump and the hydro-motor of open-circuit hydrostatic transmission (HST) system used in the mobile vehicle. The model proposed by them is a complex one and their somewhat arbitrary form makes it difficult to relate the particular loss coefficients with the physical system. Watton has developed a closed-loop design method that predicts the steady-state behavior of an axial piston hydro-motor using the test data. In his studies, a servo valve controlled hydro-motor drive system has been considered where the internal and the external losses of the drive were considered to be linear. The pressure dependence of the oil viscosity on the analysis of hydraulic system has been studied by Knezevic et al. Various loss modelling methods for hydrostatic pumps and hydro-motors are studied by Kohmascher et al. and they have introduced a new modelling method for the simulation of a state of the art HST. Murrenhoff et al. have studied the tribological behavior of the contact surfaces. Which are one of the are the main loss sources in hydrostatic units. Rahmfeld et al. have described the efficiency measurement and loss modelling of hydrostatic units and concluded that a precise measurement in combination with reliable modelling gives a useful database for designing the hydraulic system. Bergada et al. have given a complete set of the flow loss model of the slipper swash plate pair and the valve plate cylinder pair that are the main sources of the leakage in the pump, producing about 94% of the total leakage. The effect of oil temperature on losses is not considered in the said model. The effects of the operating pressure on the leakage flow characteristic of the piston type bent axis hydro-motors of different sizes have also been investigated by Kumar et al. Such studies do not consider the influences of operating temperature on the hydro-motor performance. The effects of the temperature and pressure on the leakage flow characteristic of the non-piston type positive displacement pumps have been investigated by Inaguma. The investigation presented a practical approach to predict the influence of the operating pressure and the temperature on the leakage losses in different types of hydrostatic pumps. While establishing the leakage loss model, the variation of clearances with respect to the differential pressure was also taken into consideration. The results of the said analysis are limited to the non-piston type positive displacement pumps. Using hydro-motor of bent axis design, the comparison of the performance of four types of open circuit high-speed low torque HST drives has been studied by Hasan et al. They concluded that the maximum efficiency is exhibited by HST drive having speed cont-rolled pump. The said analysis does not address the influences of the oil temperature and sizes of the hydro-motor on the drive's performance. Manring has proposed an approach for developing efficiency map for the HST drive. However, such study does not consider the effect of oil temperature and sizes of hydrostatic units (pump and motor) on the overall drive performance.

This article studies the performance of five different sizes fixed displacement bent axis hydro-motor at constant load-torque and speed at different oil temperature. The dependency of the various losses on oil temperature and the sizes of the hydro-motor are identified from the test data. Such studies have not yet been made. From the test data, various losses of the different capacities hydro-motor for a constant load torque and speed at different oil temperatures are analyzed. In analyzing the performance of the hydro-motor a model is created using bondgraph simulation technique where various losses of the motion are considered. The predicted performance parameters are obtained experimentally from the model and verified experimentally. The explicit equations defining the losses and the performance of the hydro-motors will be useful in selecting the said drive for a given application.

THE PHYSICAL SYSTEM

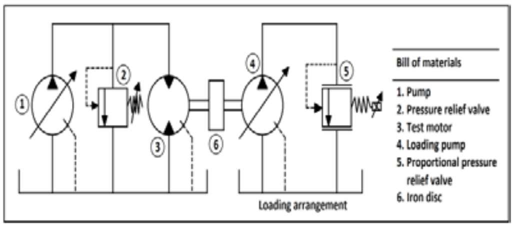

Fig. 1 The physical system

Figure 1 shows the physical system considered for analysis where a swash plate controlled variable displacement pump (1) supplies flow to drive the hydro-motor (3) at a different speed. In turn, the hydro-motor run the inertia load (6) and the loading pump (4), the flow supplied by which passes through the proportional pressure relief valve (PPRV) (5) Controlling PPRV provides load on the hydro-motor (3). By adjusting the pump displacement (4) and the set pressure of the PPRV (5), the performance of the hydro-motor (3) was tested. The pressure relief valve (2) is used to control or limit the pressure in the system. The tests were conducted for five different capacities of the hydro-motor (D_m) ranging from 10 cc/rev through 28 cc/rev and the temperature of the hydraulic oil (T) was varied from 40^0C to 80^0C. The detailed experimental set-up is discussed in Sec. 4.

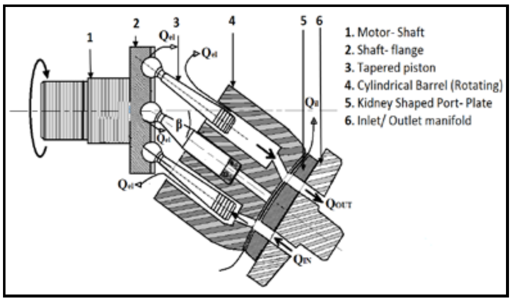

Fig. 2 Fixed displacement bent axis hydro-motor [Product Catalogue Bosch Rexroth]

The fixed displacement bent axis hydro-motor shown in fig. 2 is considered for the studies. The differential pressure across the hydro-motor ports results in inter-port leakage, termed as internal leakage (Q_{il}). Apart from this, the leakage flow also occurs due to the difference in pressure between the pumping chambers and the case drain, such leakages are termed as external leakage (Q_{el}).

MODELLING OF THE SYSTEM

The bond graph simulation technique given by Thoma is an effective tool for modelling and simulation of any physical system that consists of multi-domain. Using such technique, the system equations are easily derived from the model. Figure 3 represents the multi-bond graph model of the overall system.

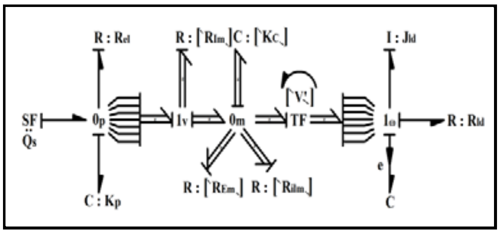

Fig. 3 Multi-bond graph model of a bent axis hydro-motor

Following assumptions are made while developing the model:

- The effects of the resistance and the capacitance of the hydraulic fluid flow passage are lumped, wherever appropriate.
- The line resistance is not taken into account.

The hydraulic power supplied to a motor gets converted into mechanical power at its drive end. In the model, a set of transformers $\left[\,^{\backslash}V'_{\backslash}\right]$represents the same. Therefore, being bilateral in nature, the TF element relates the load torque to the chamber pressure of the hydro-motor. The transformer moduli indicated by $\left[\,^{\backslash}V'_{\backslash}\right]$ represents the volumetric displacement rate (D_m) of the hydro-motor with respect to its shaft rotation.

In the multi-bond graph model, the elements SF, C and R on the 0_p junction express the inlet flow Q_s to the hydro-motor, fluid bulk stiffness K_p at the motor inlet and external leakage resistance R_{el}, respectively. The R elements that present as matrices $\left[\,^{\backslash}R_{Im_{\backslash}}\right]$ and $\left[\,^{\backslash}R_{Em_{\backslash}}\right]$ on 1_v and 0_m junctions, respectively take into account the inlet and the outlet valve-port resistances of the hydro-motor. Similarly, the resistance $\left[\,^{\backslash}R_{ilm_{\backslash}}\right]$ on 0_m junction takes into account the leakages that occur from high pressure to low- pressure chambers of the motor. The chamber fluid bulk stiffness $\left[\,^{\backslash}K_{C_{\backslash}}\right]$ is represented by C element connected to the same junction. The inertial (J_{ld}) and the frictional (R_{ld}) loads driven by the hydro-motor are taken into account by I and R elements, respectively attached to the 1_ω junction. The C element attached to the same junction is the shaft rotation observer that records the load speed.

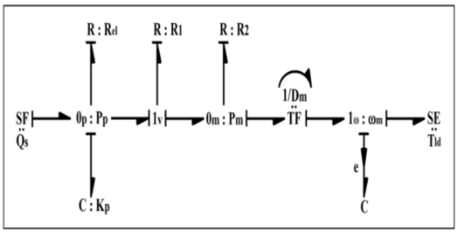

Fig. 4 Equivalent steady-state model of a bent axis hydro-motor

To analyse the system's steady-state performance from the multi-bond graph model its steady-state model is made as shown in Fig 4. In the model, R_{el} and R_1 represent the external leakage resistance and the inlet valve-port resistance, respectively. Where D_m expresses the rate of the motor displacement. In the model, all the inlet valve-ports (shown as $\left[\,^{\backslash}R_{Im_{\backslash}}\right]$ in the multi-bond graph model) is represented by R_1. Combining the resistances $\left[\,^{\backslash}R_{Em_{\backslash}}\right]$ and $\left[\,^{\backslash}R_{ilm_{\backslash}}\right]$ of the multi-bond graph model, as they are in the same junction 0_m, which are given by resistance R_2 in equivalent model. The resistances R_{el}, R_1 and R_2 may be linear or non-linear functions of the system variables and their nature are established from the experimental outcome described in Sec. 5. The resistances R_{el} and R_2 contribute hydro-motor slip whereas, R_1 accounts for the torque loss (hydro-mechanical loss) of the motor. The steady-state load torque (T_{ld}) of the hydro-motor is given by element C connected to the 1_ω junction. The chamber pressure (P_m) is caused by the load torque (T_{ld}) on the motor. Therefore in the reduced model C element on 0_m junction is not included. The model shown in Fig. 4 does not include the valve dynamics, therefore it does not present the system actual transient behaviour how the actual transient behaviour of the system. It represents the steady-state behaviour of the system fairly well. The steady-state equations obtained from the model (Fig. 4) are as givens by:

The predicted speed of the hydro-motor:

$$\omega_{mp} = \frac{\left(\frac{P_p-(T_{ld}/D_m)}{R_1} - \frac{(T_{ld}/D_m)}{R_2}\right)}{D_m} \tag{1}$$

The flow loss due to fluid compressibility:

$$Q_{cp} = Q_s - \frac{P_p}{R_{el}} - \frac{P_p-(T_{ld}/D_m)}{R_1} \tag{2}$$

Ignoring the flow loss due to fluid compressibility ($Q_{cp} = 0$) at motor inlet in steady state, the following relationships may be derived from the system's equations:

$$R_1 = \frac{P_p-(T_{ld}/D_m)}{Q_s-(P_p/R_{el})} \tag{3}$$

$$R_2 = \frac{(T_{ld}/D_m)}{-\omega_{mp}D_m+\left(\frac{P_p-(T_{ld}/D_m)}{R_1}\right)} \tag{4}$$

where, $P_p = K_p \int Q_{cp}\,dt$ (5)

Supply flow to the motor chamber through the valve-port is given by:

$$Q_m = \left(Q_s - \frac{P_p}{R_{el}}\right) \tag{6}$$

Therefore, the pressure drop due to valve-port resistance R_1 is:

$$\Delta P = \left(Q_s - \frac{P_p}{R_{el}}\right) R_1 \tag{7}$$

The hydro-motor Predicted torque-loss is expressed given by:

$$\Delta T_{lp} = \left(Q_s - \frac{P_p}{R_{el}}\right) R_1 D_m \tag{8}$$

Therefore, the predicted load torque (T_{lp}) of the motor expressed as:

$$T_{lp} = P_p D_m - \Delta T_{lp} \tag{9}$$

The predicted efficiency of the motor is expressed as follows:

$$\eta_{mp} = \frac{T_{lp}\omega_{mp}}{P_p Q_s} \tag{10}$$

As mentioned earlier, slip of the hydro-motor is due to its flow loss through the various leakage path considered as resistance R_{el} and R_2 in the model. Considering the leakage flow (the external and the internal) of the hydro-motor, the total leakage flow is given by:

$$Q_{tl} = Q_{el} + Q_{il} = \left(\frac{P_p}{R_{el}} + \frac{T_{ld}}{D_m R_2}\right) \tag{11}$$

Therefore, the predicted slip of the hydro-motor with respect to its supplied flow rate Q_s is given by:

$$S_{mp} = \left(\frac{(P_p/R_{el}) + (T_{ld}/D_m R_2)}{Q_s}\right) \tag{12}$$

The actual performance parameters of the hydro-motor are given by:

$$\eta_{ma} = \frac{T_{ld}\omega_{ma}}{P_p Q_s} \tag{13}$$

$$S_{ma} = \frac{\omega_{mi} - \omega_{ma}}{\omega_{mi}} \tag{14}$$

where, $\omega_{mi} = Q_s / D_m$ (15)

$$\Delta T_{la} = T_i - T_{ld} \tag{16}$$

where, $T_i = P_p D_m$ (17)

EXPERIMENTAL INVESTIGATION

Commercially available bent axis hydro-motor of five different capacities with seven chambers in each hydro-motor is used in the experiment. The η_o, S, and ΔT_l of the five different capacities hydro-motor (D_m) at the five different oil temperature (T) levels have been carried out experimentally using the test set-up shown in Fig. 5.

The hydro-motor performance of were determined at constant load torque and speed of 20 N m and 1100 rpm while the temperature (T) varies from 40 ^{0}C to 80 ^{0}C.

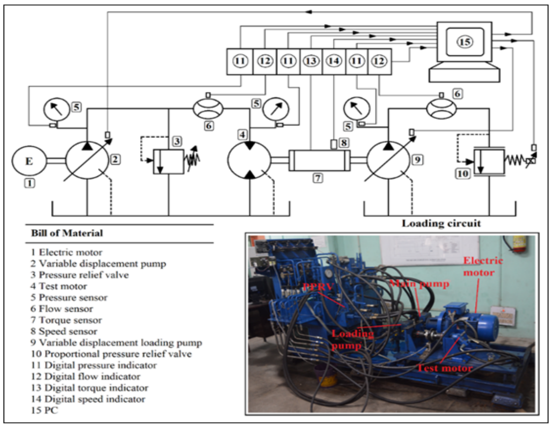

Fig. 5 Experimental set-up

A piston pump (2) rotating at a fixed speed delivers pressurised fluid to the test motor (4). The test motor (4) in turn drive the loading circuit that comprises of a pump (9) and a proportional pressure relief valve (PPRV) (10). Changing the pump flow of the loading circuit (9) by adjusting its swash plate angle or by adjusting the set pressure of PPRV (10), the hydro-motor (4) is tested at constant load torque (T_{ld}) and speed (ω_{ma}). The adjustments of the swash plate angle of the pump and the set pressure of the PPV are made through control signal that changes from 0 to 10 V dc. To record the pressure (P_p), flow (Q_s), rotational speed (ω_{ma}), oil Temperature (T) and load torque (T_{ld}) on the hydro-motor sensors along with the digital indicators are used. The tests were performed for a range of oil temperature (T), size (D_m), that vary from 40 ^{0}C to 80 ^{0}C, 10 cc/rev to 28 cc/rev and constant load torque (T_{ld}) and the hydro-motor speed (ω_{ma}) of 25 Nm and 1100 rpm, respectively. The detailed of main components used in the test set-up are listed in Table 1

Table 1 List of major components used in the test set-up

Name and specification	Model/ Make
3-Phase induction motor Power: 15 KW Speed: 1450 RPM	NADJ40224HTOP Compton Greaves Ltd.
Variable displacement main pump Maximum displacement (D_{pmax}): 28 cc/rev	A4VG28EP2DM1 / 3XRPZC10F02D / Bosch Rexroth, Germany
1. Fixed displacement hydro-motor Displacement (D_m): 10 cc/rev 2. Fixed displacement hydro-motor Displacement (D_m): 12 cc/rev 3. Fixed displacement hydro-motor Displacement (D_m): 16 cc/rev 4. Fixed displacement hydro-motor Displacement (D_m): 23 cc/rev	A2FM10 / 61W-VBB030, Bosch Rexroth, Germany A2FM12 / 61W-VBB040, Bosch Rexroth, Germany A2FM10 / 61W-VBB030, Bosch Rexroth, Germany A2FM23 / 61W-VBB030, Bosch Rexroth, Germany A2FM28 / 61W-VBB020, Bosch Rexroth, Germany

5. Fixed displacement hydro-motor Displacement (D_m): 28 cc/rev	
Variable displacement loading pump Maximum displacement (D_{pmax}): 28 cc/rev	A4VG28EP2DM1 / 3X–RPZC10F02D / Bosch Rexroth, Germany
Pressure sensor Accuracy: 0.25 % Pressure range: 0-200 bar	S10 / Wika, Germany
Flow sensor Turbine type flow sensor Accuracy: ±0.5% Flow range: 0-60 LPM	TFM 1015 / Rockwin Flow meter India Pvt. Ltd
Torque sensor Accuracy: 1% of full scale torque Max. torque range: 100 N m	K-T40B-100Q-MF-S-M-DU2-0-S / HBM, Germany
Temperature sensor Temperature measurement range: (–20 ~ 350)°C Accuracy: ±2°C	U5855A / Agilent, US

RESULTS AND DISCUSSIONS

At the onset, in evaluating the performance of the hydro-motors, its torque and the flow losses are identified that vary with the T and D_m. Using the test data of ω_{ma}, P_p, Q_s and T_{ld} in equations (2) to (4) for five different sizes of the hydro-motors, the values of R_{el}, R_1 and R_2 are obtained at five different oil temperature. The characteristics of these loss-coefficients are obtained from best fit curves lines to the data points at different D_m. The variations of such loss-coefficients with oil temperature (T) are shown in Fig. 6 through 8 and their empirical relations are given in equations (18) through (20). Using them, the effects of change of hydraulic oil temperature on the performance of different capacities of hydro-motor are studied.

Determination of the loss-coefficients (R_{el}, R_1 and R_2) of the hydro-motors

Figures 6 through 8 show the characteristics of R_{el}, R_1 and R_2 of five different capacities hydro-motor (D_m = 10 cc/rev through 28 cc/rev) at five different temperatures (T = 40^0 C through 80^0 C). These are plotted at the constant hydro-motor speed (ω_{ma}) and the load torque (T_{ld}).

The variation of R_{el} with T shown in Fig. 6 is expressed by the following empirical equation:

$$\mathrm{R_{el}} = (-3 \times 10^{-5}\,\mathrm{D_m} - 0.0004)\mathrm{T}^2 + (0.0039\,\mathrm{D_m} + 0.0077)\mathrm{T} + (0.0025\,\mathrm{D_m} + 4.936) \quad (18)$$

From Fig. 6, the following conclusions are made:

- As the oil temperature (T) increases for a constant size of the hydro-motor (D_m), the external leakage resistance (R_{el}) decreases. This occurs mainly due to decreases in the oil viscosity with increasing oil temperature which lead to the increase in the leakage flow through the clearances and hence reduces the R_{el}.
- For a constant oil temperature (T), the external leakage resistance (R_{el}) rises with rise in the capacities of the hydro-motor (D_m). This is because of the leakage flow through clearance decreases with increase in stroke length of the piston The details of such are provided in fundamental of fluid power control by Watton.

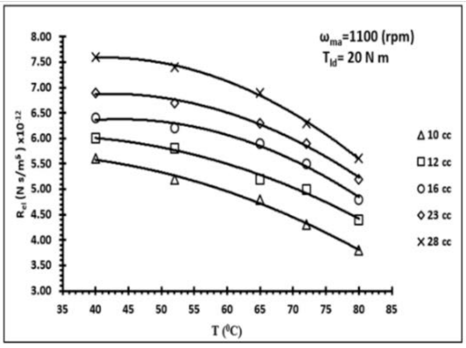

Fig. 6 External leakage resistance **(**R_{el}) characteristic of the bent axis hydro-motor

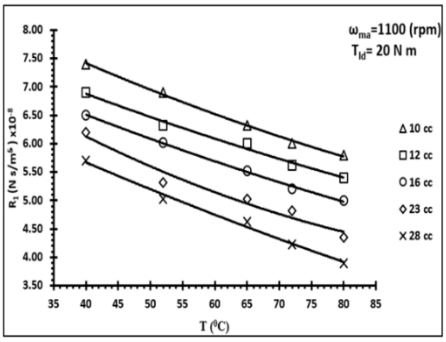

Fig. 7 Inlet valve-port resistance (R_1) characteristic of the bent axis hydro-motor

The variation of R_1 with T shown in Fig. 7 is expressed by the following empirical equation:

$$R_1 = (3 \times 10^{-6}\,D_m - 0.0001)T^2 + (-0.0006\,D_m - 0.0523)T + (-0.0678\,D_m + 9.928) \quad (19)$$

From the nature of curve shown in Fig. 7, the conclusions made are as follows:

- As the oil temperature (T) increases for a given size of the hydro-motor (D_m), inlet valve-port resistance (R_1) decreases. This is due to the effect of the oil viscosity which reduces with the rise in the oil temperature and hence lowers the R_1.
- For a constant oil temperature (T), inlet valve-port resistance (R_1) decreases with increase in the capacities of the hydro-motor (D_m) which can be observed through eq. (3)

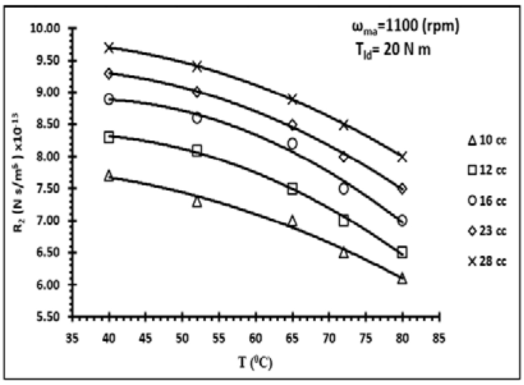

Fig. 8 Internal leakage resistance (R_2) characteristic of the bent axis hydro-motor

The variation of R_2 with T shown in Fig. 8 is expressed by the following empirical equation:

$$R_2 = (-3 \times 10^{-6}\, D_m + 0.0002)T^2 + (0.0005\, D_m - 0.0716)T + (0.0709D_m + 7.459) \tag{20}$$

The following conclusions are made from the nature of curve shown in Fig. 8:

- As the oil temperature (T) increases for a constant size of the hydro-motor (D_m), the R_2 decreases. This occurs mainly due to decreasing nature of the oil viscosity with the increase in the oil temperature which increases the leakage flow through the clearances and hence reduces the R_2.
- For a constant oil temperature (T), the internal leakage resistance (R_2) rises with the increase in the capacities of the hydro-motor (D_m). This is because of the leakage flow through clearances decreases with increase in stroke length of the piston. The details of such are provided in fundamental of fluid power control by Watton.

The decrease in the resistances R_{el} and R_2 of the hydro-motor raises the flow-loss (slip) due to which volumetric efficiency of the hydro-motor decreases whereas, the torque-loss of the hydro-motor rises with the rise in the inlet valve-port resistance (R_1) which results in lower the hydro-mechanical efficiency.

Determination of slip of the hydro-motors

Using the characteristics of the resistances (R_{el} and R_2) given by equations (18) and (20) in equation (12), the predicted slip of the five different sizes hydro-motor at five different oil temperature is obtained. The actual and predicted slip is compared as shown in Fig. 9.

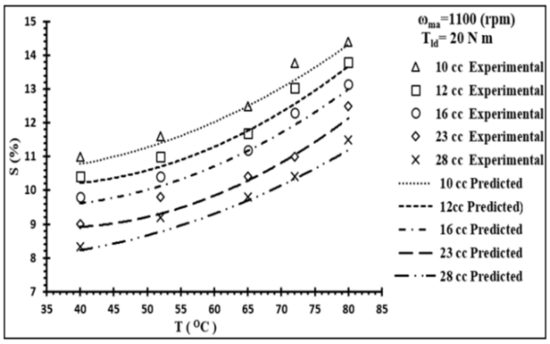

Fig. 9 Slip characteristic of the bent axis hydro-motor

The conclusions made from Fig. 9 are as follows:

- For a given D_m, the slip of the hydro-motor rises with the increase in the oil temperature (T). This is due reason that the external leakage resistance (R_{el}) and the internal leakage resistance (R_2) both are decreasing with rising temperature as shown in figs. 6 and 8.
- As the size of the hydro-motor (D_m) increases, the slip decreases for a constant oil temperature (T). This is due to the reason that the external leakage resistance (R_{el}) and the internal leakage resistance (R_2) both are increases with increasing D_m as shown in figs. 6 and 7.

Determination of torque loss of the hydro-motors

Torque loss of the hydro-motor depends on the R_1. Using the characteristics of R_1 given by equation (19) in equation (8), the predicted torque-loss (%) of the five different sizes hydro-motor at five different oil temperature is obtained. They are compared with the actual torque-loss (%) obtained through the test data by using equation (16) and are shown in Fig. 10.

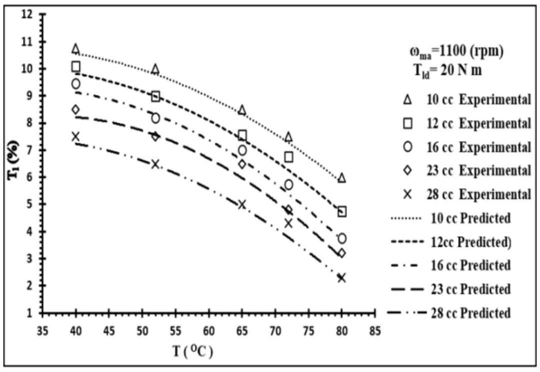

Fig. 10 Torque loss characteristic of the bent axis hydro-motor

From the characteristics shown in Fig. 10, the following observations are made:

- For a specific size of the hydro-motor (D_m), with the rise in the oil temperature (T), the torque-loss (%) decreases. This is because of the inlet valve-port resistance (R_1) decreases with the increasing oil temperature as shown in fig. 7. Also, due to the decrease in the viscosity of oil with increasing temperature which lead to reduce the viscous friction and hence reduce the torque loss (%).
- As the size of the hydro-motor increases (D_m), the torque-loss (%) decreases for a given oil temperature (T). This is because the inlet valve-port resistance (R_1) decreases with the increase in the size of the hydro-motor as shown in fig. 7.

Determination of hydro-motors overall efficiency

The overall efficiency of the hydro-motor depends on the slip and the torque-loss. Slip and the torque-loss depend on the various losses (R_{el}, R_1 and R_2) of the hydro-motor. Using the characteristics of such losses given by equations (18) through (20) in equation (10), the predicted overall efficiency of the five different sizes hydro-motor at five different oil temperature is obtained. They are compared with the actual efficiency obtained through the test data by using equation (13) and are shown in Fig. 11.
The following conclusions are made from the characteristics illustrated in Fig. 11:

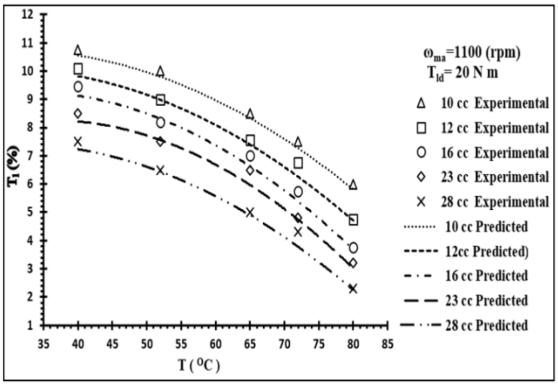

Fig. 11 Overall efficiency of the bent axis hydro-motor

- For a fixed size of the hydro-motor (D_m), the overall efficiency increases with the increase in the oil temperature (T). This is due to the decreasing nature of the percentage of torque loss with rising temperature as shown in fig. 10.
- At a given oil temperature (T), with the increase in the D_m, the overall efficiency also increases. This is due to the decreasing nature of the slip and the torque-loss (%) with increasing D_m as shown in fig. 9 and 10.

It is observed that the actual value is lower by 2% to 3% compares to the predicted values calculated from the equation obtained from the model. Therefore, the nature of the loss-coefficients shows by equations (18) through (20) is acceptable in evaluating the hydro-motor performances.
The generalized equation for the overall efficiency of the different capacities fixed displacement bent axis hydro-motor at different oil temperatures and the constant load torque and speed is given below:

$$\eta_O = (3\times10^{-5}\,D_m + 4\times10^{-5})T^2 + (-0.0023\,D_m + 0.0116)T + (0.326\,D_m + 76.47) \qquad (21)$$

By using equation (21), the values of overall performance of the different capacities fixed displacement hydro-motor at different oil temperature can be found.

CONCLUSIONS

In this article, the performance of five different sizes of the bent axis hydro-motor at five different temperatures and for a given operating condition has been investigated. The following conclusions are drawn from the study of five different size bent axis hydro-motors at a constant load of 20 N m and speed of 1100 rpm.

- For a specific size of the hydro-motor, with rise in the temperature, the slip increases while the percentage of torque loss decreases and the overall efficiency of the hydro-motor increase.
- As the size of the hydro-motor increases for a constant oil temperature, the torque-loss in percentage and the slip decreases while the overall efficiency of the hydro-motors increases.

The authors believe that this method of predicting the performance may be useful to the practicing engineers and it may also be helpful for selection of hydro-motor for a particular demand of load and speed in Heavy vehicle system, mining industries and construction equipment. Also, such method may be helpful in determining the characteristics of the losses and the performance parameters of the hydro-motor without disassembling the said unit (motor).

Further studies on the effect of the pressure and temperature on hydraulic oil density and its effects on the hydro-motors overall performance need to be established. Studies in this regards may be a potential future work.

REFERENCES

Bergada, J.M., Davies, D.L. Kumar, S. and Watton, J. The effect of oil pressure and temperature on barrel film thickness and barrel dynamics of an axial piston pump. *Meccanica* 2012; 47(3): 639-654.

Hasan, M.E., Dasgupta, K. and Ghoshal, S. Comparison of the efficiency of the high speed low torque hydrostatic drives using bent axis motor: An experimental study. *Proc IMechE,* *Part E: Journal of Process Mechanical Engineering* 2015; 231(4): 650-666.

Inaguma, Y. A practical approach for analysis of leakage flow characteristics in hydraulic pumps. *Proc IMechE Sci, Part C: J Mechanical Engineering Science* 2013; 227(5): 980-991.

Knežević, D. and Savić, V. Mathematical modeling of changing of dynamic viscosity, as a function of temperature and pressure of the mineral oils for hydraulic systems. *Mechanical Engineering, Facta Universities*, 2006; 4(1): 27-34.

Kohmäscher, T., Rahmfeld, R., Murrenhoff, H. and S. Eckhard. Improved loss modeling of hydrostatic units - Requirement for precise simulation of mobile working machine drivelines. In: *Proceedings of the International Mechanical Engineering Congress and Exposition*, Seattle, Washington, USA, 11-15 Nov., 2007, pp. 41803-14.

Kumar, N., Dasgupta, K. and Ahmad, F. Analysis of leakage flow characteristics in bent axis hydro-motors. In: *Proceedings of the 1st International and 16th National Conference on Machines and Mechanisms*, IIT Roorkee, India, 18-20 Dec, 2013, pp. 18-20.

Manring, N.D. Mapping the efficiency for a hydrostatic transmission. *J Dynamic System, Measurement and Control* 2016; 138(3): 031004-8.

Murrenhoff, H., Piepenstock, U. and Kohmäscher, T. Analyzing losses in hydrostatic drives. In: *Proceedings of the 7th International Symposium on Fluid Power*, Aachen ,Germany, Sep. 15-18, 2008, pp. 103-107.

Product catalogue of the bent axis piston hydro-motor RE 91 001/09.00, Bosch Rexroth India Ltd.

Rahmfeld, R and Skirde, E. Efficiency measurement and modelling – essential for optimizing hydrostatic systems. In: *Proceedings of the 7th International fluid power conference*, Aachen, Germany, 22-24 March, 2010, 2, pp.1-14.

Thoma, J U. Simulation by Bond graph. Berlin: *Springer*, 1990.

Watton, J. An explicit design approach to determine the optimum steady state performance of axial piston hydro-motor drives. *Proc IMechE, Part I: J Systems and Control Engineering* 2006; 220(2): 131-143.

Watton, J. Fundamentals of fluid power control. 1st ed. UK: *Cambridge University Press*, 2009.

Zarotti, L.G and Paoluzzi, R. In quest of the transmission size. In: *Proceedings of the 3rd JFPS International Symposium on Fluid Power*, Cassana-Ferrara, Italy, 1996, 3, pp. 295-300.

NOTATIONS

ω_{ma} Hydro-motor's actual speed
ω_{mi} Hydro-motor's ideal speed
ω_{mp} Hydro-motor's predicted speed
P_p Plenum pressure of the hydro-motor
P_m Chamber pressure of the hydro-motor
D_m Size of the hydro-motor
T_{ld} Load torque on the hydro-motor
T_i Ideal torque of the hydro-motor
T_{lp} Hydro-motor's predicted torque
T Temperature of the hydraulic oil in ^oC
R_{el} Plenum leakage resistance of the hydro-motor
R_1 Inlet valve-port resistance of the hydro-motor
R_2 Internal leakage resistance of the hydro-motor
Q_{cp} Compressibility of the fluid in the plenum
Q_m Supply flow to the motor chamber
Q_s Flow supplied to the hydro-motor
Q_{el} External leakage flow of the hydro-motor
Q_{il} Internal leakage flow of the hydro-motor
Q_{tl} Total leakage flow of the hydro-motor
K_p Effective bulk stiffness of the plenum fluid
ΔT_{la} Hydro-motor's actual torque-loss
ΔT_{lp} Hydro-motor's predicted torque-loss
S_{ma} Actual slip of the hydro-motor output shaft
S_{mp} Predicted slip of the hydro-motor output shaft
η_{ma} Actual overall efficiency of the hydro-motor
η_{mp} Predicted overall efficiency of the hydro-motor
$\left[{}^{\backslash}R_{Im\backslash} \right]$ Inlet valve-port resistance (diagonal matrix)
$\left[{}^{\backslash}R_{Em\backslash} \right]$ Outlet valve-port resistance (diagonal matrix)
$\left[{}^{\backslash}R_{ilm\backslash} \right]$ Inter-chamber leakage resistance (diagonal matrix)
$\left[{}^{\backslash}K_{C\backslash} \right]$ Equivalent bulk stiffness of the chamber fluid (diagonal matrix)